

SCIENTIFIC REPORTS



OPEN

Characterization of a novel low-temperature-active, alkaline and sucrose-tolerant invertase

Junpei Zhou^{1,2,3,4,*}, Limei He^{2,*}, Yajie Gao², Nanyu Han^{1,2,3,4}, Rui Zhang^{1,2,3,4}, Qian Wu^{1,2,3,4}, Junjun Li^{1,2,3,4}, Xianghua Tang^{1,2,3,4}, Bo Xu^{1,2,3,4}, Junmei Ding^{1,2,3,4} & Zunxi Huang^{1,2,3,4}

Received: 28 May 2016
Accepted: 02 August 2016
Published: 24 August 2016

A glycoside hydrolase family 32 invertase from *Bacillus* sp. HJ14 was expressed in *Escherichia coli*. The purified recombinant enzyme (rInvHJ14) showed typical biochemical properties of low-temperature-active and alkaline enzymes: (i) rInvHJ14 was active and stable in the range of pH 7.0–9.5 with an apparent pH optimum of 8.0; (ii) rInvHJ14 was most active but not stable at 30–32.5 °C, with 19.7, 48.2 and 82.1% of its maximum activity when assayed at 0, 10 and 20 °C, respectively, and the E_a , ΔG^\ddagger (30 °C), K_m (30 °C) and k_{cat} (30 °C) values for hydrolysis of sucrose by rInvHJ14 was 47.6 kJ mol⁻¹, 57.6 kJ mol⁻¹, 62.9 mM and 746.2 s⁻¹, respectively. The enzyme also showed strong sucrose tolerance. rInvHJ14 preserved approximately 50% of its highest activity in the presence of 2045.0 mM sucrose. Furthermore, potential factors for low-temperature-active and alkaline adaptations of rInvHJ14 were presumed. Compared with more thermostable homologs, rInvHJ14 has a higher frequency of glycine residues and a longer loop but a lower frequency of proline residues (especially in a loop) in the catalytic domain. The catalytic pockets of acid invertases were almost negatively charged while that of alkaline rInvHJ14 was mostly positively charged.

Sucrose can be hydrolyzed by invertases (EC 3.2.1.26) into an equimolar mixture of D-glucose and D-fructose. Invertases, also termed as β -fructofuranosidase and sucrase, fall into glycoside hydrolase (GH) family 32 based on their amino acid sequences homology¹. Invertases are of great interest in basic research and various industrial applications especially in food industry². These enzymes are used for the preparation of invert sugar, high fructose syrup, jams, candies, soft centered chocolates and cookies, creams, marshmallows, powder milk for infants, artificial honey and beverages items². In addition to sucrose, some invertases also hydrolyze fructose-containing oligosaccharides and fructans, such as raffinose^{3–7}, stachyose^{8,9}, kestose^{10,11}, nystose^{10,11}, inulin^{2,11–13} and levan¹⁴.

It is well-known that low temperatures strongly inhibit the rates of enzyme-catalysed reactions. Low-temperature-active enzymes are the exceptions because they can show high catalytic activity at low temperatures associated with low stability at intermediate and high temperatures¹⁵. These properties are of relevance to applications in industries as diverse as food, household detergents, aquaculture, bioremediation, tanning, energy, pharmaceutical and molecular biology¹⁶. For example, low-temperature-active enzymes can be used in food industry for meat tenderizing, cheese ripening, dough fermentation, wine and beverage stabilization, and clarification of fruit, vegetable juices and wine¹⁶. Low temperatures avoid spoilage and change in nutritional value and flavour of the original heat-sensitive substrates and products¹⁶. Biotechnological processes performed at low temperatures can also provide economic benefit by reducing energy consumption¹⁶. Furthermore, low-temperature-active enzymes are important to maintain the metabolic rates and sustained growth compatible with life in cold ecosystems that actually occupy over 85% of the Earth's surface¹⁵. However, low-temperature-active invertase has not been reported to date.

¹Engineering Research Center of Sustainable Development and Utilization of Biomass Energy, Ministry of Education, Yunnan Normal University, Kunming, 650500, People's Republic of China. ²College of Life Sciences, Yunnan Normal University, Kunming, 650500, People's Republic of China. ³Key Laboratory of Yunnan for Biomass Energy and Biotechnology of Environment, Yunnan, Kunming, 650500, People's Republic of China. ⁴Key Laboratory of Enzyme Engineering, Yunnan Normal University, Kunming, 650500, People's Republic of China. *These authors contributed equally to this work. Correspondence and requests for materials should be addressed to Z.H. (email: huangzunxi@163.com)

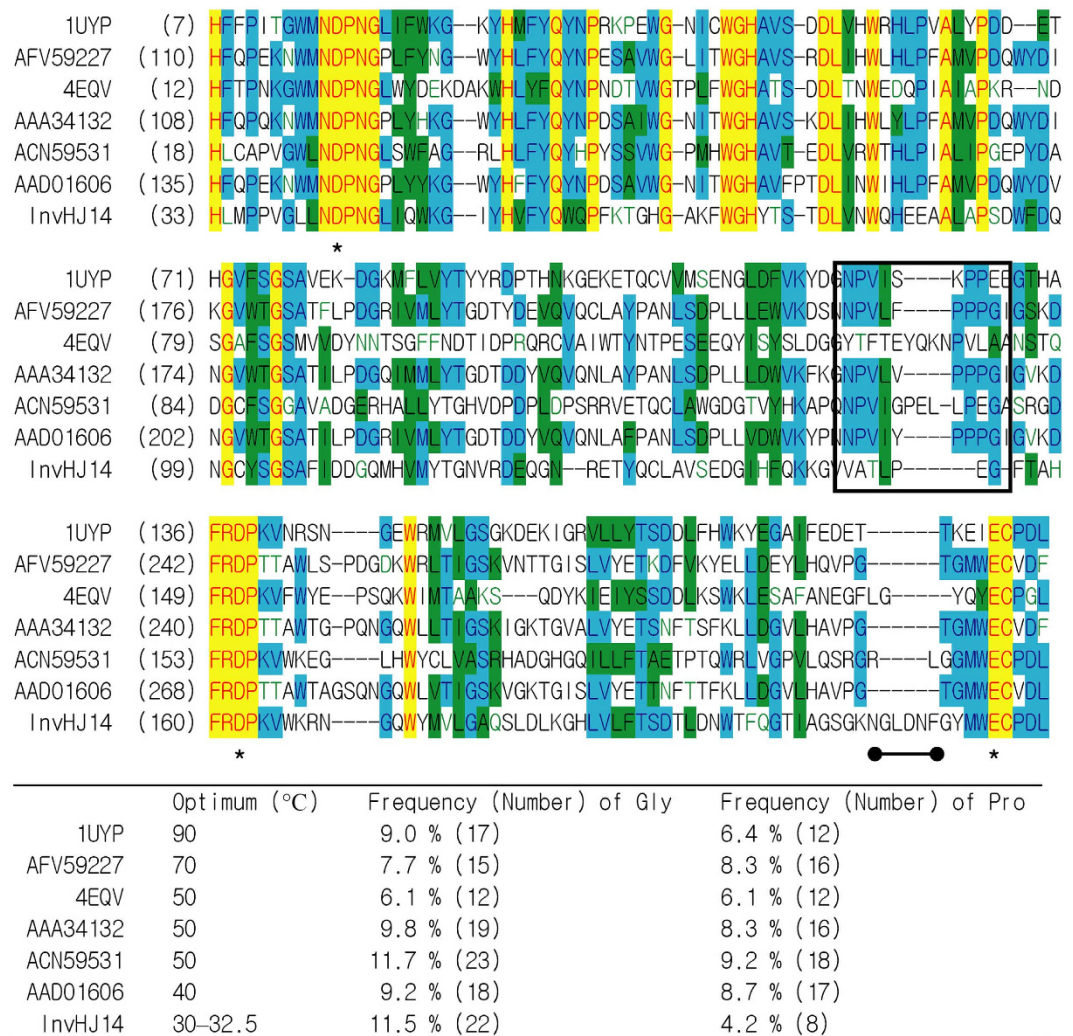


Figure 1. Partial amino acid sequence alignment of InvHJ14 with mesophilic and thermophilic GH 32 invertases. The invertases include InvTM from *T. maritima* (Accession No. or PDB ID: 1UYP)¹³, InvEH from *E. haichowensis* (AFV59227)³⁸, InvSC from *S. cerevisiae* (4EQV)²⁷, InvSL from *S. lycopersicum* (AAA34132)³⁹, InvUB from an uncultured bacterium (ACN59531)²⁴ and InvIB from *I. batatas* (AAD01606)²⁸. Asterisks show the putative active residues. The segment corresponding to V149–G155 of InvHJ14, which presents the difference of proline residues between InvHJ14 and more thermostable homologs, is *framed*. The amino acid residues N210 to F215 of InvHJ14, which build a longer loop in Fig. 2, are *underlined*.

Invertases have been isolated from a variety of sources, including bacteria¹⁷, yeast¹², fungi¹⁰, higher plants¹⁸ and animals¹⁹. Acid invertases have been the most extensively studied and isolated from various sources while much less is known about alkaline invertases which have been reported only from plants and cyanobacteria^{2,4,5,20–24}.

In this study, a new GH 32 invertase, designated InvHJ14, was discovered from *Bacillus* sp. HJ14. The enzyme was expressed in *Escherichia coli* and the recombinant enzyme was purified. The recombinant InvHJ14 (rInvHJ14) was tolerant to sucrose and showed typical properties of low-temperature-active and alkaline enzymes. The potential molecular adaptations to low-temperature and alkaline environments of the enzyme were presumed.

Results

Sequence analysis. A gene of 1,458 bp encoding putative invertase of 55.9 kDa was predicted from the draft genome of HJ14. *In silico* analysis indicated that the invertase lacked recognizable signal peptide sequence but was comprised of a catalytic domain of GH 32 from H33 to P339 and a C-terminal domain of GH 32 from K338 to Q480. The consensus pattern of GH 32, H-x(2)-[PV]-x(4)-[LIVMA]-N-D-P-N-[GA] (<http://prosite.expasy.org/PS00609>), was also detected in InvHJ14 (HLMPPVGLLNDPNG in Fig. 1). The residues D43, D162 and E220 are the predicted nucleophile, transition-state stabilizer and general acid/base catalyst, respectively (Fig. 1)^{11,25}.

A BLASTP search against NCBI protein database showed that InvHJ14 was most similar to a number of putative invertases translated from genome sequences. In the result, InvHJ14 was found to have the maximal sequence identity of 99.6% with the uncharacterized GH 32 invertase from *Bacillus safensis* JPL_MERTA8-2

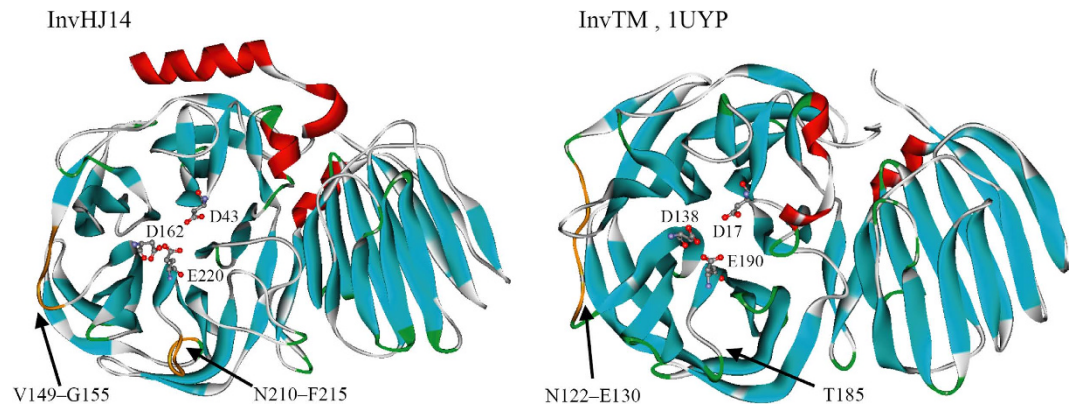


Figure 2. Structures of low-temperature-active InvHJ14 and the thermophilic invertase InvTM. InvTM is a *T. maritima* invertase (Accession No. or PDB ID: 1UYYP) which shows optimal activity at 90 °C¹³. The putative active residues are detailed in ball-and-stick form. Arrows indicate loops built by V149–G155 and N210–F215 of InvHJ14 and the corresponding amino acid residues of InvTM as shown in Fig. 1.

(WP_046312845). Furthermore, the BLASTP analysis showed that InvHJ14 had 45.6% identity with the experimentally characterized GH 32 invertase (SurA) from *Geobacillus stearothermophilus* NUB36 (AAB38976)¹⁷.

Structure analysis. The acidic invertases InvSC from *Saccharomyces cerevisiae* (Accession No. or PDB ID: 4EQV), InvIB from *Ipomoea batatas* (AAD01606), InvTM from *Thermotoga maritima* (1UYYP), InvBL from *Bifidobacterium longum* (3PIJ) and InvUB from an uncultured bacterium (ACN59531) exhibit optimal activities at pH 4.8, pH 5.0, pH 5.5, pH 6.2 and pH 6.5, respectively^{13,24,26–28}. The model of InvIB was built using the crystal structure of a GH 32 β -fructofuranosidase from *Arabidopsis thaliana* (PDB ID: 2QQV) as the template with a sequence similarity of 42% and a GMQE score of 0.63. Models of InvUB and InvHJ14 were built using the crystal structure of InvBL as the template (Fig. 2), with sequence similarities of both 36% and GMQE scores of 0.67 and 0.66, respectively. As shown in Fig. 3, catalytic pockets of these invertases presented different surface charges. The catalytic pockets of acidic InvSC, InvIB, InvTM, InvBL and InvUB were almost negatively charged, while the opposite was observed for InvHJ14.

Expression, purification and identification of rInvHJ14. rInvHJ14 was successfully expressed in *E. coli* BL21 (DE3), extracted by cell lysis using sonication, and purified by Ni²⁺-NTA metal chelating affinity chromatography. A clear single band (approximately 58 kDa) representing the recombinant invertase was seen on the SDS–PAGE (Fig. S1). MALDI–TOF MS spectrum of the band matched the molecular masses of internal peptides from rInvHJ14 (Fig. S2), confirming that the purified enzyme is indeed rInvHJ14.

Substrate specificity. Determined at pH 8.0 and 30 °C, the specific activities of purified rInvHJ14 toward 0.5% (w/v) sucrose, raffinose and fructooligosaccharides mixture were 155.1 ± 1.5 , 4.5 ± 0.1 and 3.1 ± 0.3 U mg^{−1}, respectively. However, no activity of rInvHJ14 was detected toward substrate of 0.5% (w/v) sucralose, stachyose, levan, inulin, starch, birchwood xylan, beechwood xylan, wheat flour arabinoxylan or *p*-nitrophenyl- β -D-xylopyranoside.

Biochemical characterization. Purified rInvHJ14 had activity in the range of pH 7.0–9.5 with an apparent pH optimum of 8.0 (Fig. 4a). Over 85% of its initial activity was observed after incubating the enzyme for 1 h in buffers with pH 7.0–9.0 (Fig. 4b). The apparent optimal temperature for rInvHJ14 was in the range from 30 to 32.5 °C (Fig. 4c). The enzyme could retain 48.2 and 82.1% of its maximum activity when assayed at 10 and 20 °C, respectively (Fig. 4c). At the temperature of 0 °C, invertase activity of 19.7% was even retained (Fig. 4c). Half-lives of the enzyme were approximately 30 and 10 min when assayed at 30 and 37 °C, respectively (Fig. 4d).

Addition of 1.0 mM MnSO₄ and β -mercaptoethanol slightly enhanced the activity of rInvHJ14, but addition of CuSO₄, HgCl₂ and SDS strongly or completely inhibited the enzyme activity. The presence of other metal ions and chemical reagents had little or no effect on the enzyme activity (Table S1).

The activity of rInvHJ14 increased with the increase in sucrose concentration from 14.6 mM to 876.4 mM (Fig. 5). Then, rInvHJ14 was inhibited by the substrate at concentration of higher than 876.4 mM (Fig. 5). rInvHJ14 preserved approximately 50% of its highest activity in the presence of 2045.0 mM sucrose (Fig. 5).

Kinetic and thermodynamic characterization. From the Arrhenius plots (Fig. 6), the E_a value for hydrolysis of sucrose by rInvHJ14 was 47.6 kJ mol^{−1}. The Q_{10} value (20 °C and 30 °C) for the hydrolysis of sucrose by rInvHJ14 was 1.9. Other kinetic and thermodynamic values are summarized in Table 1.

Transglycosylation activity. Self-condensation or transglycosylation product was not observed for rInvHJ14 in this study (Fig. S3).

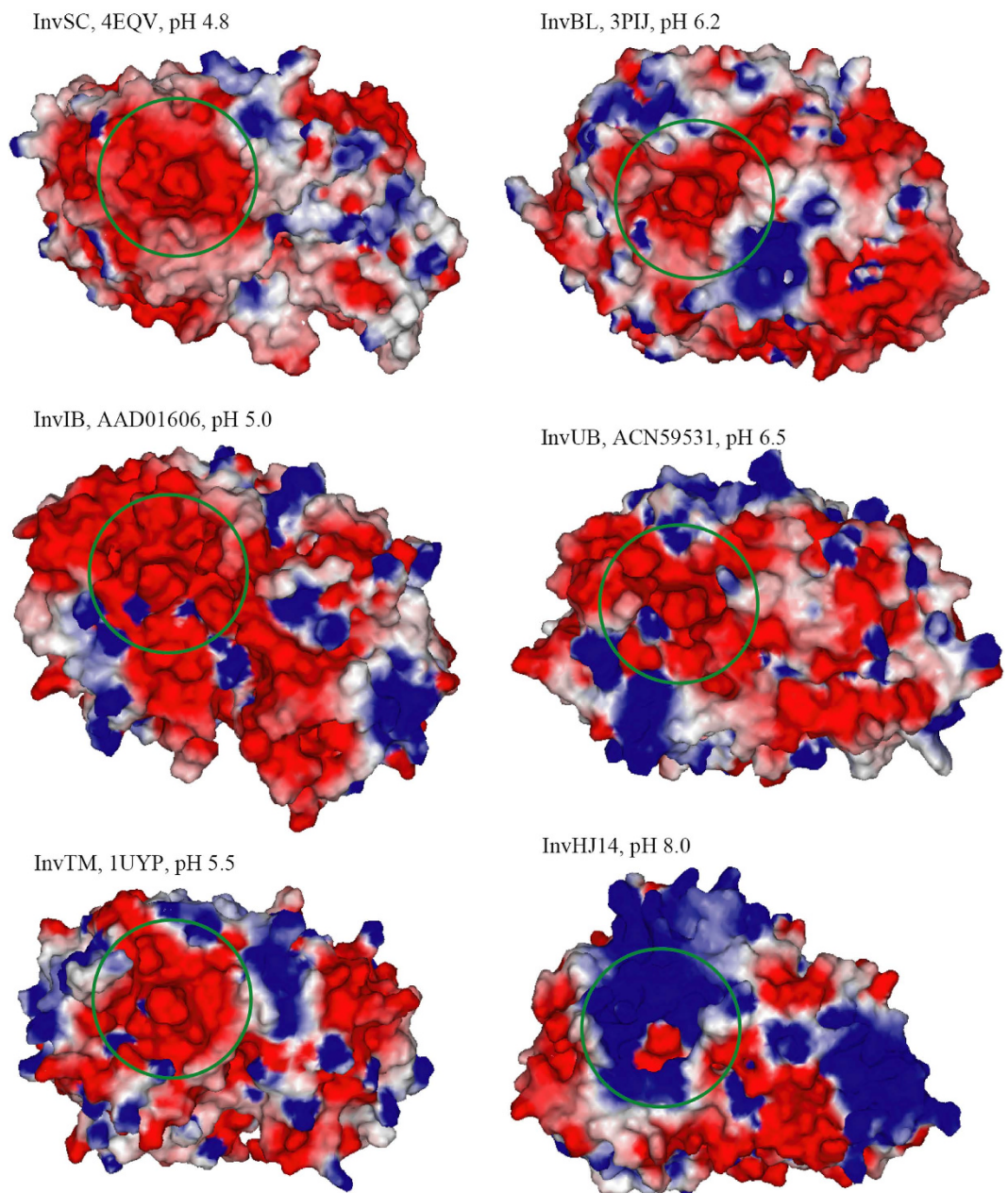


Figure 3. Charge distributions on the surfaces of GH 32 invertases with acidic and alkaline pH optima. The invertases include InvSC from *S. cerevisiae* (Accession No. or PDB ID: 4EQV)²⁷, InvIB from *I. batatas* (AAD01606)²⁸, InvTM from *T. maritima* (1UYYP)¹³, InvBL from *B. longum* (3PIJ)²⁶ and InvUB from an uncultured bacterium (ACN59531)²⁴. Catalytic pockets are circled. Charge distribution on the surface was calculated at pH 7.0. Positive charges are depicted in blue and negative charges in red.

Discussion

rInvHJ14 shows typical properties of low-temperature-active enzymes as its optimal activity is 30–32.5 °C, it has high catalytic activity at 0 and 10 °C, and it is thermolabile at 30 °C or higher temperatures¹⁵. Compared with rInvHJ14, most invertases show properties of mesophilic or thermophilic enzymes as their optimal activities are at temperatures of equal to or higher than 45 °C, they are thermostable at 50 °C or higher than 50 °C, and they show no activity or less than 10% relative activity at 10 °C^{2,3,7,8,12,18,24,28–35}. The kinetic and thermodynamic properties of rInvHJ14 further indicate that the invertase is a low-temperature-active enzyme. Many low-temperature-active enzymes have lower E_a values than their more thermostable homologs because E_a decreases with a decrease in ΔG^\ddagger or a decrease in energy barriers which allow easy conformational changes of enzymes during catalysis at low temperatures^{36,37}. The E_a and ΔG^\ddagger values for hydrolysis of sucrose by rInvHJ14 was 47.6 kJ mol⁻¹ and 57.6 kJ mol⁻¹, respectively, which are lower than the values for some thermostable invertases, such as *Saccharum officinarum* L. invertase showing an optimal temperature of 55 °C with an E_a value of 55.3 kJ mol⁻¹ and a ΔG^\ddagger value of 71.2 kJ mol⁻¹¹⁸, *Fusarium* sp. invertase showing an optimal temperature of 50 °C

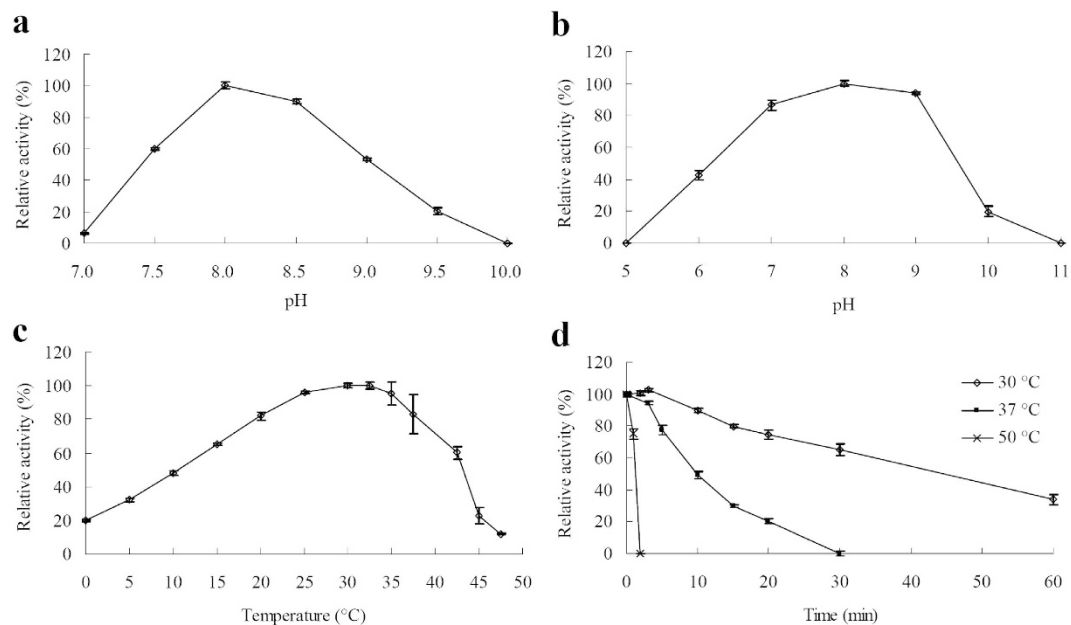


Figure 4. Enzymatic properties of purified rInvHJ14. (a) pH-dependent activity profiles. **(b)** pH stability assay. **(c)** Temperature-dependent activity profiles. **(d)** Thermostability assay. Error bars represent the means ± SD (n = 3).

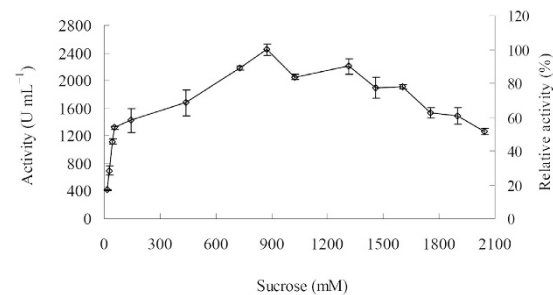


Figure 5. The effect of sucrose on purified rInvHJ14. Error bars represent the means ± SD (n = 3).

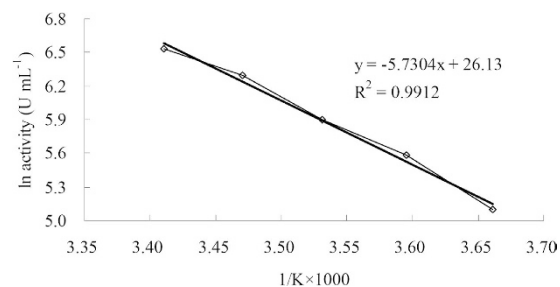


Figure 6. Arrhenius plot for the determination of E_a for sucrose hydrolysis by purified rInvHJ14.

and an E_a value of 72.4 kJ mol^{-1} ³⁵, and *Oryza sativa* invertase showing an E_a value of $100.8 \text{ kJ mol}^{-1}$ ⁹. The majority of low-temperature-active enzymes have higher K_m and k_{cat} values than their thermostable counterparts in order to decrease the activation free-energy barrier³⁶. rInvHJ14 has higher K_m (62.9 mM) and k_{cat} (746.2 s^{-1}) values than some thermostable invertases, such as *Elsholtzia haichowensis* invertase showing an optimal temperature of 70°C with a K_m value of 2.68 mM and a k_{cat} value of 469.17 s^{-1} ³⁸, *Kluyveromyces marxianus* invertase showing an optimal temperature of $50\text{--}55^\circ\text{C}$ with a K_m value of 2.5 mM and a k_{cat} value of 301 s^{-1} ¹², and many microbial invertases with K_m values of lower than 60 mM as reviewed previously².

Catalytic domains of many low temperature-active enzymes present more number of glycine residues but less number of proline residues especially in loops than their more thermostable homologs because glycine residues

Parameters	10 °C	20 °C	30 °C
K_m (mM)	50.3	57.6	62.9
V_{max} ($\mu\text{mol min}^{-1} \text{mg}^{-1}$)	231.7	599.7	771.5
k_{cat} (s^{-1})	224.1	580.0	746.2
k_{cat}/K_m ($\text{mM}^{-1} \text{s}^{-1}$)	4.4	10.1	11.9
ΔG° (kJ mol^{-1})	56.5	56.2	57.6
ΔH° (kJ mol^{-1})	45.3	45.2	45.1
ΔS° ($\text{J mol}^{-1} \text{K}^{-1}$)	-39.4	-37.6	-41.1

Table 1. Kinetic and thermodynamic characterization of purified rInvHJ14 toward sucrose.

can provide localized chain mobility but proline residues restrict backbone rotations^{15,16}. That will generate enhanced flexible region surrounding the catalytic site and finally allow catalysis of enzymes at low temperatures^{15,16}. As shown in Fig. 1, InvHJ14 has more number or higher frequency of glycine residues but less number or lower frequency of proline residues in the catalytic domain from conserved HXXXXXXXXNDPNG to ECXXX than some mesophilic and thermophilic invertases. The number or frequency of glycine residues in the catalytic domain of InvHJ14 is approximately 2-fold compared with that of the invertase InvSC. On the contrary, the numbers or frequencies of proline residues in the catalytic domains of the invertases InvIB, InvUB, InvSL from *Solanum lycopersicum* (AAA34132)³⁹ and InvEH from *E. haichowensis* (AFV59227)³⁸ are around 2-fold compared with that of InvHJ14. And the numbers or frequencies of proline residues in the catalytic domains of the invertases InvSC and InvTM are approximately 1.5-fold compared with that of InvHJ14. Notably, proline residues in most mesophilic and thermophilic invertases increase significantly in the segment corresponding to V149–G155 of InvHJ14 as shown in Fig. 1. These amino acid residues in the segment build a loop near the predicted transition-state stabilizer D162 (Fig. 2). Consequently, the increased number of glycine residues combined with the decreased number of proline residues allow easier local conformational changes of InvHJ14 and finally contribute to low-temperature adaptation of the enzyme.

The amplitude of the movement between secondary structures can be increased by longer loop then result in the higher structure flexibility¹⁶. InvHJ14 has an increased number of amino acid residues from N210 to F215 compared with some mesophilic and thermophilic invertases (Fig. 1). These amino acid residues build a longer loop which is close to the catalytic E220 (Fig. 2). As such, the proper plasticity close to the catalytic site enables rInvHJ14 maintaining high catalytic activity at low temperatures accompanied by thermolability at intermediate and high temperatures.

rInvHJ14 is an alkaline invertase as it shows activity and stability at alkaline conditions. To our knowledge, alkaline invertases have been reported only from plants and cyanobacteria^{2,4,5,20–24}. Most invertases produced by microorganisms worked optimally in the range of pH 2.9–6.2². As such, the study is the first to report an alkaline invertase isolated from eubacteria. Compared with their acidic counterparts, alkaline enzymes have a larger positively charged surface to keep them active and stable under alkaline condition, such as the alkaline β -mannanase from *Humicola insolens* Y1⁴⁰ and α -galactosidase from *Streptomyces* sp. HJG4³⁷. In this study, structure analysis found that the catalytic pockets of acidic InvSC, InvIB, InvTM, InvBL and InvUB were almost negatively charged while that of alkaline InvHJ14 was mostly positively charged. Therefore, a positively charged catalytic pocket is presumed to be a factor for alkaline adaptation of the GH 32 invertase rInvHJ14.

Furthermore, enzymatic hydrolysis of sucrose is preferable in the production of high-quality inverted syrups compared with acidic hydrolysis⁴¹. A high sucrose content; even as high as 2 M, is used in the industrial application⁴¹. As such, the identification of an invertase that is active in the presence of 2 M sucrose is relevant. It has been reported that the commercial invertase from *S. cerevisiae* displayed approximately 30% of its highest activity at 2 M sucrose⁴². The invertases from a metagenomic library and *Aspergillus niger* show approximately 50%²⁴ and 30%¹⁰ of their highest activities at 1 M sucrose, respectively. In the presence of 2 M sucrose, the yeast *Candida guilliermondii* MpIIIa invertases INV3a-N and INV3a-D present nearly 50% and 10% of their highest activities, respectively⁷. Similar to INV3a-N, rInvHJ14 remained approximately 50% of its highest activity in the presence of 2045.0 mM sucrose. The big differences between INV3a-N and rInvHJ14 are that INV3a-N is an acidic and thermophilic invertase⁷. Together, rInvHJ14 may be a potential candidate for enzymatic hydrolysis of sucrose in the production of high-quality inverted syrups.

In conclusion, a GH 32 invertase was isolated from an eubacteria—*Bacillus* sp. HJ14. Biochemical characterization revealed that the enzyme was a novel low-temperature-active, alkaline and sucrose-tolerant invertase. These characteristics make the invertase suitable for versatile applications, especially in the food industry. Moreover, molecular characterization of the enzyme contributes to a better understanding of the structure–function relationships of low-temperature-active and alkaline invertases.

Materials and Methods

Strains, vectors and reagents. The details of isolation, identification and preservation of *Bacillus* sp. HJ14 were described in our previous study⁴³.

E. coli BL21 (DE3) and pEASY-E2 vector (TransGen, Beijing, China) were used for gene expression. Ni²⁺-NTA agarose (Qiagen, Valencia, CA, USA) was used to purify the recombinant protein. Genomic DNA and plasmid isolation kits were purchased from Tiangen (Beijing, China). DNA polymerases (*Taq* and *Pyrobest*) and dNTPs were purchased from TaKaRa (Otsu, Japan). Sucrose, birchwood xylan, beechwood xylan, *p*-nitrophenyl- β -D-xylopyranoside, inulin from dahlia tubers (I3754), raffinose, starch, D-glucose, D-galactose,

D-fructose and D-xylose were purchased from Sigma–Aldrich (St. Louis, MO, USA). Wheat flour arabinoxylan (P-WAXYM) was purchased from Megazyme (Wicklow, Ireland). Stachyose and sucralose were purchased from Tokyo Chemical Industry (Tokyo, Japan). Fructooligosaccharides set including kestose, nystose and fructofuranosyl-nystose was purchased from Wako Pure Chemical (Osaka, Japan). Levan from *Zymomonas mobilis* was purchased from Advanced Technology & Industrial (Hong Kong, China), Isopropyl- β -D-1-thiogalactopyranoside (IPTG) was purchased from Amresco (Solon, OH, USA). Silica gel G plates were purchased from Haiyang (Qingdao, China). All chemicals were of analytical grade.

Gene cloning and sequence analysis. The genome of HJ14 was sequenced on a HiSeq 2000 sequencer (Illumina) and genomic data was analyzed on a NF supercomputing server (Inspur, Shandong, China) in our lab. Other details are as described in our previous study⁴³.

Genes from the draft genome of HJ14 were predicted by the tools GeneMark.hmm 2.8 (http://exon.gatech.edu/GeneMark/gmhmm2_prok.cgi) combined with local BLAST 2.2.25⁴⁴. The identity values of DNA and protein sequences were obtained from the BLASTN and BLASTP (<http://www.ncbi.nlm.nih.gov/BLAST/>) results, respectively. The signal peptide and catalytic domain were predicted by SignalP (<http://www.cbs.dtu.dk/services/SignalP/>) and InterPro online tool (<http://www.ebi.ac.uk/interpro/>), respectively.

Structure analysis. Tertiary structures of invertases were predicted by homology modeling using SwissModel (<http://swissmodel.expasy.org/>). Spatial distributions of electrostatic potential of tertiary structures were calculated using the Discovery Studio 2.5 software (Accelrys, San Diego, CA, USA).

Heterologous expression. The InvHJ14-encoding gene (*invHJ14*) was amplified by PCR using *Pyrobest* DNA polymerase and the primer set *rinvHJ14EF* (ATGACAACACTACTGACGCAGC) and *rinvHJ14ER* (TTGATCTGCTTCTCTTTGTAAAT), and then the resulting PCR product was added base A at the 5' terminal using *rTaq* DNA polymerase. The recombinant plasmid, designated *pEASY-invHJ14*, was constructed with *invHJ14* and *pEASY-E2* vector through T-A ligation and transformed into *E. coli* BL21 (DE3) competent cells. The positive transformant harboring *pEASY-invHJ14* was identified by PCR analysis and confirmed by DNA sequencing. The overnight culture of positive transformant was inoculated (1:100 dilutions) into fresh Luria–Bertani medium containing 100 μ g mL⁻¹ ampicillin, and incubated at 37 °C. Upon reaching an OD_{600nm} of 0.7, 0.7 mM IPTG was added to the broth to induce enzyme expression at 20 °C for further 20 h.

Purification and identification of recombinant enzyme. *E. coli* cells were collected by centrifugation at 10,000 \times g at room temperature for 5 min. The resulting cell pellet was resuspended in sterilized, ice-cold buffer A (20 mM Tris–HCl, 0.5 M NaCl, pH 7.2), and sonicated on ice with 100 short bursts for 4 s each at a power output of 150 W. The suspension was centrifuged at 10,000 \times g at room temperature for 5 min then the precipitation was removed. The supernatant was collected and passed over Ni²⁺-NTA agarose gel columns previously equilibrated with buffer A. Stepwise elution was carried out with buffer A containing 0, 20, 40, 60, 80, 100, 200, 300 and 500 mM imidazole, in that order. Eluted fractions containing enzyme activity were collected and stored at –20 °C until used for subsequent analyses.

For determination of protein purity after Ni²⁺-NTA purification, eluted fractions were loaded for sodium dodecyl sulfate–polyacrylamide gel electrophoresis (SDS–PAGE) using 12% running gels. The purified protein in the SDS–PAGE gel was identified using matrix-assisted laser desorption/ionization time-of-flight mass spectrometry (MALDI–TOF MS) performed by Tianjin Biochip (Tianjin, China). The protein concentration was determined with Bradford method using bovine serum albumin as the standard⁴⁵.

Enzyme assay and substrate specificity. The sucrose hydrolysis reactions involved incubations at 37 °C for 10 min with a reaction mixture containing 100 μ L of appropriately diluted rInvHJ14 and 900 μ L of McIlvaine buffer (pH 8.0) containing 0.5% (w/v) sucrose. The amount of reducing sugars released was determined by the 3,5-dinitrosalicylic acid (DNS) reagent at 540 nm⁴⁶. One activity unit (U) was defined as the amount of enzyme that produces 1.0 μ mol equimolar mixture of glucose and fructose per minute under the above assay conditions unless otherwise noted.

Substrate specificity assay was performed at 37 °C in McIlvaine buffer (pH 8.0) using 0.5% (w/v) sucralose, raffinose, stachyose, levan, inulin, starch, birchwood xylan, beechwood xylan, wheat flour arabinoxylan or fructooligosaccharides mixture as substrate instead of sucrose. Enzyme catalysis on *p*-nitrophenyl- β -D-xylopyranoside was assayed using the method described in the previous study⁴³.

Biochemical characterization. Biochemical characterization of purified rInvHJ14 was determined using sucrose as substrate unless otherwise noted.

The effects of pH and temperature on rInvHJ14 were determined at pH 7.0–10.0 and 0–50 °C, respectively. pH and temperature stabilities of rInvHJ14 were studied respectively by keeping the enzyme solution at 37 °C for 60 min at different pH values (pH 5.0–11.0) and by keeping the enzyme solution at pH 8.0 for 1–60 min at different temperatures (30–50 °C). Residual activities of these pre-incubated samples were then determined under standard assay conditions. The buffers used were McIlvaine buffer for pH 5.0–8.5 and 0.1 M glycine–NaOH for pH 9.0–11.0.

Various metal ions and chemical reagents were individually added to the reaction solution to investigate their effects on rInvHJ14. These metal ions and chemical reagents were 1.0 mM (final concentration) NaCl, KCl, CaCl₂, CoCl₂, NiSO₄, CuSO₄, MgSO₄, MnSO₄, ZnSO₄, Pb(CH₃COO)₂, HgCl₂, FeCl₃, EDTA, β -mercaptoethanol and SDS, and 1.0% (v/v) Tween 80 and Triton X-100. Any precipitation was removed by centrifugation before measuring the absorption.

In order to determine whether the activity of rInvHJ14 was inhibited by sucrose at high final concentrations, the enzyme was incubated in the reaction mixture with 14.6–2045.0 mM sucrose. Enzyme activity was then determined under standard assay conditions.

Kinetic and thermodynamic characterization. K_m , V_{max} and k_{cat} values of purified rInvHJ14 were determined using 1.5–36.5 mM sucrose as substrate in McIlvaine buffer (pH 8.0) at 10, 20 and 30 °C. The data were plotted according to the Michaelis–Menten method using the computer software GraphPad Prism (GraphPad Software, San Diego, CA, USA).

The activation energy (E_a), free energy of activation (ΔG^\ddagger), enthalpy of activation (ΔH^\ddagger), entropy of activation (ΔS^\ddagger) and temperature coefficient (Q_{10}) for rInvHJ14 were calculated using the equations as described in previous study⁴⁷.

Transfructosylating reactions. In order to determine whether rInvHJ14 possessed self-condensation activity, the enzyme (approximately 0.5 U mL⁻¹) was incubated in the reaction mixture with 146 or 584 mM sucrose at 20 °C and pH 8.0 for 17 h. Transglycosylation reactions were carried out at 20 °C and pH 8.0 for 17 h using 146 mM sucrose as the donor with D-galactose and D-xylose as the acceptors at 555 mM and 666 mM, respectively. Transglycosylation products were analyzed by thin layer chromatography (TLC) as previously described³⁷.

Accession number. Nucleotide sequence of *invHJ14* was deposited in GenBank under the accession number KT943473.

References

- Lombard, V., Ramulu, H. G., Drula, E., Coutinho, P. M. & Henrissat, B. The carbohydrate-active enzymes database (CAZy) in 2013. *Nucleic Acids Res* **42**, D490–D495 (2014).
- Nadeem, H. *et al.* Microbial invertases: a review on kinetics, thermodynamics, physicochemical properties. *Process Biochem* **50**, 1202–1210 (2015).
- Chowdhury, S. *et al.* Characterization of a novel low molecular weight sucrose from filamentous fungus *Termitomyces clypeatus*. *Process Biochem* **44**, 1075–1082 (2009).
- Morell, M. & Copeland, L. Enzymes of sucrose breakdown in soybean nodules—alkaline invertase. *Plant Physiol* **74**, 1030–1034 (1984).
- Matsushi, K. & Uritani, I. Change in invertase activity of sweet potato in response to wounding and purification and properties of its invertases. *Plant Physiol* **54**, 60–66 (1974).
- Aguiar, T. Q. *et al.* Molecular and functional characterization of an invertase secreted by *Ashbya gossypii*. *Mol Biotechnol* **56**, 524–534 (2014).
- Plascencia-Espinosa, M. *et al.* Effect of deglycosylation on the properties of thermophilic invertase purified from the yeast *Candida guilliermondii* MpIIIa. *Process Biochem* **49**, 1480–1487 (2014).
- Rubio, M. C., Runco, R. & Navarro, A. R. Invertase from a strain of *Rhodotorula glutinis*. *Phytochemistry* **61**, 605–609 (2002).
- Isla, M. I., Salerno, G., Pontis, H., Vattuone, M. A. & Sampietro, A. R. Purification and properties of the soluble acid invertase from *Oryza sativa*. *Phytochemistry* **38**, 321–325 (1995).
- Goosen, C. *et al.* Molecular and biochemical characterization of a novel intracellular invertase from *Aspergillus niger* with transfructosylating activity. *Eukaryot Cell* **6**, 674–681 (2007).
- Alvaro-Benito, M., Polo, A., Gonzalez, B., Fernandez-Lobato, M. & Sanz-Aparicio, J. Structural and kinetic analysis of *Schwanniomyces occidentalis* invertase reveals a new oligomerization pattern and the role of its supplementary domain in substrate binding. *J Biol Chem* **285**, 13930–13941 (2010).
- Aziz, S. *et al.* Hyperproduction and thermal characterization of a novel invertase from a double mutant derivative of *Kluyveromyces marxianus*. *Food Technol Biotech* **49**, 465–473 (2011).
- Alberto, F., Bignon, C., Sulzenbacher, G., Henrissat, B. & Czjzek, M. The three-dimensional structure of invertase (β -fructosidase) from *Thermotoga maritima* reveals a bimolecular arrangement and an evolutionary relationship between retaining and inverting glycosidases. *J Biol Chem* **279**, 18903–18910 (2004).
- Quiroga, E. N., Vattuone, M. A. & Sampietro, A. R. Purification and characterization of the invertase from *Pycnoporus sanguineus*. *BBA-Protein Struct M* **1251**, 75–80 (1995).
- Feller, G. & Gerday, C. Psychrophilic enzymes: hot topics in cold adaptation. *Nat Rev Microbiol* **1**, 200–208 (2003).
- Cavicchioli, R. *et al.* Biotechnological uses of enzymes from psychrophiles. *Microbial Biotechnology* **4**, 449–460 (2011).
- Li, Y. & Ferenci, T. The *Bacillus stearothermophilus* NUB36 *surA* gene encodes a thermophilic sucrose related to *Bacillus subtilis* SacA. *Microbiol-SGM* **142**, 1651–1657 (1996).
- Hussain, A., Rashid, M. H., Perveen, R. & Ashraf, M. Purification, kinetic and thermodynamic characterization of soluble acid invertase from sugarcane (*Saccharum officinarum* L.). *Plant Physiol Bioch* **47**, 188–194 (2009).
- Heil, M., Buchler, R. & Boland, W. Quantification of invertase activity in ants under field conditions. *J Chem Ecol* **31**, 431–437 (2005).
- Vargas, W., Cumino, A. & Salerno, G. L. Cyanobacterial alkaline/neutral invertases. Origin of sucrose hydrolysis in the plant cytosol? *Planta* **216**, 951–960 (2003).
- Yao, Y. *et al.* Genome-wide identification, expression, and activity analysis of alkaline/neutral invertase gene family from Cassava (*Manihot esculenta* Crantz). *Plant Mol Biol Rep* **33**, 304–315 (2015).
- Lee, H. S. & Sturm, A. Purification and characterization of neutral and alkaline invertase from carrot. *Plant Physiol* **112**, 1513–1522 (1996).
- Kulshrestha, S., Tyagi, P., Sindhi, V. & Yadavilli, K. S. Invertase and its applications—a brief review. *J Pharm Res* **7**, 792–797 (2013).
- Du, L. Q., Pang, H., Hu, Y. Y., Wei, Y. T. & Huang, R. B. Expression and characterization in *E. coli* of a neutral invertase from a metagenomic library. *World J Microb Biot* **26**, 419–428 (2010).
- Chuanhayan, P. *et al.* Crystal structures of *Aspergillus japonicus* fructosyltransferase complex with donor/acceptor substrates reveal complete subsites in the active site for catalysis. *J Biol Chem* **285**, 23249–23262 (2010).
- Bujacz, A., Jedrzejczak-Krzepkowska, M., Bielecki, S., Redzynia, I. & Bujacz, G. Crystal structures of the apo form of β -fructofuranosidase from *Bifidobacterium longum* and its complex with fructose. *FEBS J* **278**, 1728–1744 (2011).
- Sainz-Polo, M. A. *et al.* Three-dimensional structure of *Saccharomyces* invertase: role of a non-catalytic domain in oligomerization and substrate specificity. *J Biol Chem* **288**, 9755–9766 (2013).
- Huang, W. C., Wang, A. Y., Wang, L. T. & Sung, H. Y. Expression and characterization of sweet potato invertase in *Pichia pastoris*. *J Agr Food Chem* **51**, 1494–1499 (2003).

29. Bhatti, H. N., Asgher, M., Abbas, A., Nawaz, R. & Sheikh, M. A. Studies on kinetics and thermostability of a novel acid invertase from *Fusarium solani*. *J Agr Food Chem* **54**, 4617–4623 (2006).
30. Liebl, W., Brem, D. & Gotschlich, A. Analysis of the gene for β -fructosidase (invertase, inulinase) of the hyperthermophilic bacterium *Thermotoga maritima*, and characterisation of the enzyme expressed in *Escherichia coli*. *Appl Microbiol Biot* **50**, 55–64 (1998).
31. Akgol, S., Kacar, Y., Denizli, A. & Arica, M. Y. Hydrolysis of sucrose by invertase immobilized onto novel magnetic polyvinylalcohol microspheres. *Food Chem* **74**, 281–288 (2001).
32. Chaudhuri, A. & Maheshwari, R. A novel invertase from a thermophilic fungus *Thermomyces lanuginosus*: its requirement of thiol and protein for activation. *Arch Biochem Biophys* **327**, 98–106 (1996).
33. Giraldo, M. A. *et al.* Thermostable invertases from *Paecilomyces variotii* produced under submerged and solid-state fermentation using agroindustrial residues. *World J Microb Biot* **28**, 463–472 (2012).
34. Belcarz, A., Ginalska, G., Lobarzewski, J. & Penel, C. The novel non-glycosylated invertase from *Candida utilis* (the properties and the conditions of production and purification). *BBA-Protein Struct M* **1594**, 40–53 (2002).
35. Shaheen, I., Bhatti, H. N. & Ashraf, T. Production, purification and thermal characterisation of invertase from a newly isolated *Fusarium* sp. under solid-state fermentation. *Int J Food Sci Tech* **43**, 1152–1158 (2008).
36. Siddiqui, K. S. & Cavicchioli, R. Cold-adapted enzymes. *Annu Rev Biochem* **75**, 403–433 (2006).
37. Zhou, J. P. *et al.* Characterization of two glycoside hydrolase family 36 α -galactosidases: novel transglycosylation activity, lead-zinc tolerance, alkaline and multiple pH optima, and low-temperature activity. *Food Chem* **194**, 156–166 (2016).
38. Xu, Z. R., Liu, C., Cai, S. W., Zhang, L. & Xiong, Z. T. Heterologous expression and comparative characterization of vacuolar invertases from Cu-tolerant and non-tolerant populations of *Elsholtzia haichowensis*. *Plant Cell Rep* **34**, 1781–1790 (2015).
39. Tautzin, A. S. *et al.* Functional characterization of a vacuolar invertase from *Solanum lycopersicum*: post-translational regulation by N-glycosylation and a proteinaceous inhibitor. *Biochimie* **101**, 39–49 (2014).
40. Luo, H. Y. *et al.* Gene cloning, expression, and biochemical characterization of an alkali-tolerant β -mannanase from *Humicola insolens* Y1. *J Ind Microbiol Biot* **39**, 547–555 (2012).
41. Krastanov, A. Continuous sucrose hydrolysis by yeast cells immobilized to wool. *Appl Microbiol Biot* **47**, 476–481 (1997).
42. Vasquez-Bahena, J., Montes-Horcasitas, M. C., Ortega-Lopez, J., Magana-Plaza, I. & Flores-Cotera, L. B. Multiple steady states in a continuous stirred tank reactor: an experimental case study for hydrolysis of sucrose by invertase. *Process Biochem* **39**, 2179–2182 (2004).
43. Zhou, J. P. *et al.* A thermo-halo-tolerant and proteinase-resistant endoxylanase from *Bacillus* sp. HJ14. *Folia Microbiol* **59**, 423–431 (2014).
44. Altschul, S. F., Gish, W., Miller, W., Myers, E. W. & Lipman, D. J. Basic local alignment search tool. *J Mol Biol* **215**, 403–410 (1990).
45. Bradford, M. M. A rapid and sensitive method for the quantitation of microgram quantities of protein utilizing the principle of protein-dye binding. *Anal Biochem* **72**, 248–254 (1976).
46. Miller, G. L. Use of dinitrosalicylic acid reagent for determination of reducing sugar. *Anal Chem* **31**, 426–428 (1959).
47. Siddiqui, K., Cavicchioli, R. & Thomas, T. Thermodynamic activation properties of elongation factor 2 (EF-2) proteins from psychrotolerant and thermophilic Archaea. *Extremophiles* **6**, 143–150 (2002).

Acknowledgements

This work was supported by National Natural Science Foundation of China (No. 31460694), Yunling Scholars (No. 2015-56), Yunling Industry Leading Talents (No. 2014-1782), Reserve Talents Project for Young and Middle-Aged Academic and Technical Leaders of Yunnan Province (No. 2015HB033) and Applied and Basic Research Foundation of Yunnan Province (Nos 2013FZ045 and 201401PC00224).

Author Contributions

J.Z. conceived of the idea, designed the experiments, performed data analysis and wrote the manuscript; L.H. and Y.G. performed the experiments; N.H. and R.Z. helped perform data analysis; Q.W., J.L., X.T., B.X. and J.D. coordinated the study; Z.H. conceived of the idea, designed the experiments and coordinated the study. All authors discussed the results, reviewed and approved the final manuscript.

Additional Information

Supplementary information accompanies this paper at <http://www.nature.com/srep>

Competing financial interests: The authors declare no competing financial interests.

How to cite this article: Zhou, J. *et al.* Characterization of a novel low-temperature-active, alkaline and sucrose-tolerant invertase. *Sci. Rep.* **6**, 32081; doi: 10.1038/srep32081 (2016).



This work is licensed under a Creative Commons Attribution 4.0 International License. The images or other third party material in this article are included in the article's Creative Commons license, unless indicated otherwise in the credit line; if the material is not included under the Creative Commons license, users will need to obtain permission from the license holder to reproduce the material. To view a copy of this license, visit <http://creativecommons.org/licenses/by/4.0/>

© The Author(s) 2016